

Effect of Mn Concentration on the Structural and Optical Properties of SnO₂ Thin Films Prepared By pulse laser deposition

Kadhim .A .Aadim,*Ramiss .A . Alansary and *Sally .A. Alhady

Baghdad University, College of Science Physics Department

**Baghdad University, College of Science for Women Physics Department*

Abstract: Tin oxide doped (SnO₂:Mn) films have been deposited on glass substrates by pulsed laser deposition. SnO₂ is a wide band gap n-type semi-conductor that has a wide range of applications. Mn doped SnO₂ semi-conducting transparent thin films were prepared by pulse laser deposition under different doped (Mn) concentration. XRD results showed that the films had polycrystalline nature with tetragonal rutile structure. Furthermore, we have also investigated the Optical Transmission Spectra of the films such as refractive index (n) and extinction coefficient (k). The calculated refractive indexes of the films with various Mn concentrations were in the range of 1.8 to 2.1. The extinction coefficient, k was found to be very small. The energy gap value was decreased with increasing doping concentration.

Keywords: tin oxide, pulse laser deposition, energy band gap

I. Introduction

Study of SnO₂ transparent conducting oxide thin films are of great interest due to its unique attractive properties like high optical transmittance, uniformity, good electrical, low resistivity, chemical inertness, stability to heat treatment, mechanical hardness, Piezoelectric behavior and its low cost. SnO₂ thin films have vast applications as window layers, heat reflectors in solar cells, flat panel display, electro-chromic devices, LEDs, liquid crystal displays, invisible security circuits, various gas sensors etc. Undoped and Mn doped SnO₂ thin films have been prepared by pulse laser deposition technique and reported that SnO₂ belongs to n-type semiconductor with a direct optical band gap of about 4.08 eV [1]. Doped tin oxide (SnO₂) films have been widely used as transparent conducting electrodes in many optoelectronic and electro-optic devices such as solar cells [2,3] and flat panel displays [4,5] due to their high electrical conductivity and high optical transmittance in the visible, and high infrared reflectance. There are numerous deposition techniques used to grow SnO₂ films (either doped or undoped) including chemical vapor deposition (CVD) [6,7], spray pyrolysis [8,9], thermal evaporation [10], sol-gel [11] and sputtering [12,13,14]. Other techniques, such as pulsed laser deposition (PLD) might be used to achieve high-quality SnO₂ films; however, the growth of Mn-doped SnO₂ films by PLD has not yet been reported. PLD films crystallize at relatively lower substrate temperatures compared to other physical vapor deposition (PVD) processes due to the high kinetic energies (N1 eV) of the ejected species in the laser produced plasma [15-17]. In this work we study the effect of (Mn) on the structural and optical properties of SnO₂.

II. Experimental

The deposition was carried out using a Q switched Nd:YAG laser at 1064 nm (1000 shot and laser fluency 700mJ/cm²). The studied films were prepared from pure SnO₂ and doped Mn targets films were grown by pulsed laser deposition on glass substrates kept distance of 1 cm from the SnO₂ target. For film deposition, All substrates (the glass substrates with 1 mm thickness and 8 × 2.5 cm²), were cleaned in acetone and methanol solutions in an ultrasonic bath for 30 minutes. Then compress the mixture under 5 Ton (homemade compressor) to get the final pellet of Tin Oxide powder and tin doped (Mn) of 2.5 cm diameter. The structural properties of the films were analyzed by X-ray diffraction (XRD, Cu Kα1, λ = 0.154 nm) and The optical properties of the films were studied at room temperature with a UV-VIS spectrometer in the wavelength range of 200- 800 nm was analyzed to determine the refractive index and energy gap value for each sample.

III. Results and discussion:

Fig (1-a) shows the X-ray diffraction patterns for undoped SnO₂ and SnO₂: Mn films grown on glass substrates at 473 K. It can be seen that all the films are polycrystalline and contain the SnO₂ tetragonal structure [18].

Doping concentration is one of the main parameters, which determine the structural properties of the films. The crystalline size of as deposited films were calculated using Scherrer's formula given by,

$$D = \frac{0.9\lambda}{\beta \cos \theta} \dots \dots \dots (1)$$

Where λ is the wavelength of X-ray used (1.54 Å), β is the full width half maximum (FWHM) of the peak and θ is the glancing angle. The calculated crystalline size (D) of Mn doped Tin oxide are tabulated in table 1. SnO₂ films doped with (Mn) with (30,40 and 50 %) under 10⁻² mbar Oxygen pressure at 473 K annealing temperature and 700mJ/cm² laser fluence glass from fig notes that At 30 wt% concentration, showed diffraction peaks located at $2\theta=26.5897^\circ$, $2\theta=33.8799^\circ$, $2\theta=37.9553^\circ$, $2\theta=41.2523^\circ$, and $2\theta=51.7766^\circ$, corresponding to the (110), (101), (200), (101) and (211) peaks respectively. By increasing doping at 40wt% concentration, showed diffraction peaks located at $2\theta=26.6057^\circ$, $2\theta=33.8959^\circ$, $2\theta=37.9713^\circ$, $2\theta=41.2524^\circ$ and $2\theta=51.7926^\circ$, corresponding to the (110),(101),(200),(101) and (211) peaks respectively. At 50% wt% concentration, showed diffraction peaks located at $2\theta=26.6167^\circ$, $2\theta=33.9069^\circ$ and $2\theta=41.2525^\circ$ corresponding to the (110),(101) and (101) where the peaks position of the plane was shifted to high 2θ values with increasing amounts of Mn content. It has been reported that the c-axis bond of Mn doped with SnO₂ lattice was increased as the doping increased due to the replacement of the Mn ions were substituted into the Sn⁺ in the lattice of SnO₂ film. Therefore; the peak intensities increased [19,20] the FWHM of SnO₂ doping with Mn decreases with increasing concentration of doping. The FWHM and the grain size of the samples are shown in table1. A point of interest is that the preferential orientation is the (110) direction of the films, this may be due to the layer stability of the (110) planes which reflects the more relaxed bonds with minimum energy. Another interpretation is that this stability originates in the larger density of bonds [21]. It is clear that there were little shifting of 2θ location to higher values and an increase of the peaks intensity accompanied the increasing of sulfide content in prepared samples as given in Table (1).

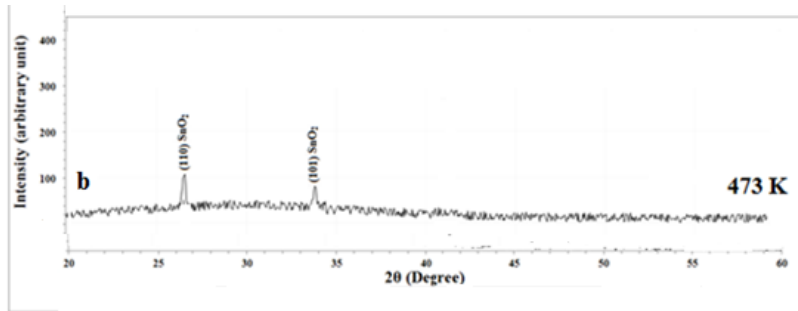


Fig (1-a): XRD of SnO₂ thin films pure at 473 K

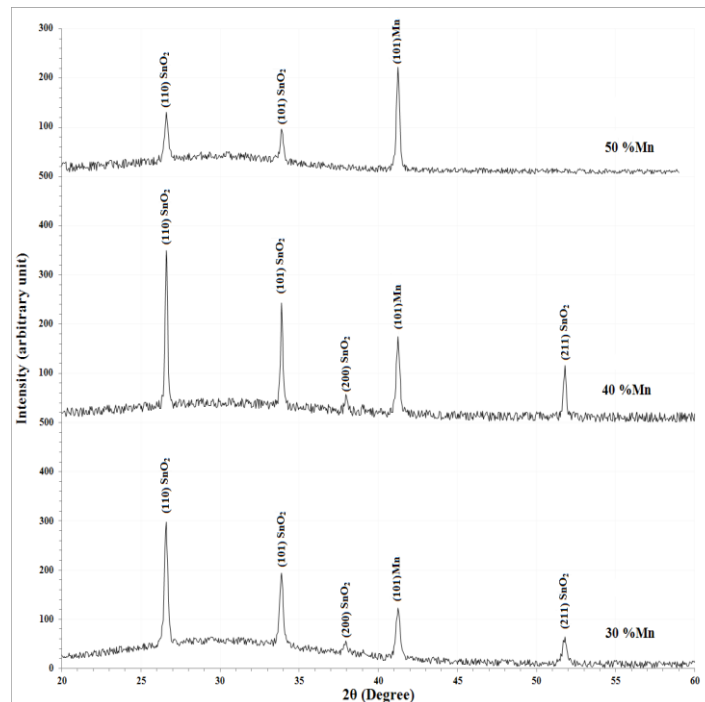
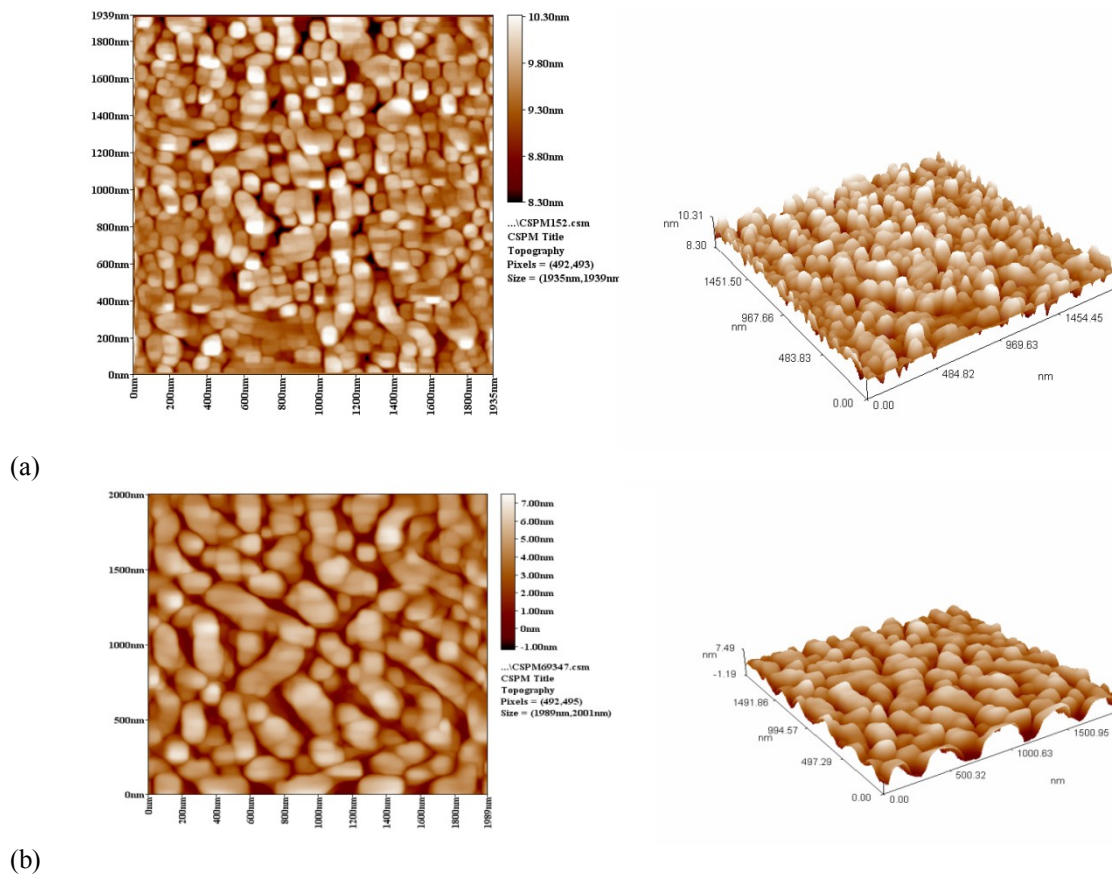


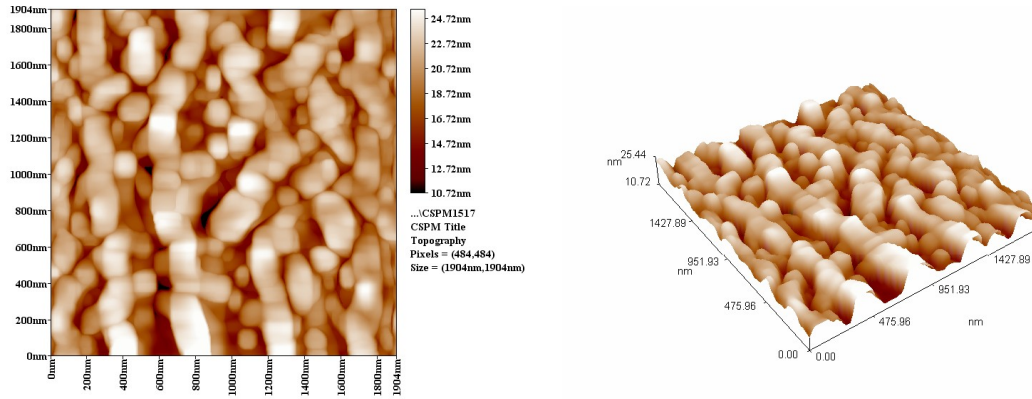
Fig (1-b) XRD of SnO₂:Mn thin film (30, 40 and 50)% concentration Mn with annealing temperature 473k a- SnO₂:30 %Mn b-SnO₂:40 %Mn c- SnO₂:50 %Mn

T _a (K)	Mn%	2θ (Deg.)	FWHM (Deg.)	Int. (Arb.U.)	d _{hkl} Exp. (Å)	hkl	Phase	d _{hkl} Std. (Å)	G.S (Å)
473	30	26.5897	0.2295	296	3.3497	(110)	SnO ₂	3.3503	335
		33.8799	0.2445	191	2.6437	(101)	SnO ₂	2.6441	320
		37.9553	0.2595	31	2.3687	(200)	SnO ₂	2.3690	305
		41.2523	0.3416	122	2.1867	(101)	Mn	2.1871	234
		51.7766	0.3045	64	1.7642	(211)	SnO ₂	1.7644	273
	40	26.6057	0.1532	346	3.3477	(110)	SnO ₂	3.3503	502
		33.8959	0.1633	241	2.6425	(101)	SnO ₂	2.6441	479
		37.9713	0.1734	54	2.3677	(200)	SnO ₂	2.3690	456
		41.2524	0.3036	173	2.1867	(101)	Mn	2.1871	263
		51.7926	0.2032	115	1.7637	(211)	SnO ₂	1.7644	409
	50	26.6167	0.2321	98	3.3463	(110)	SnO ₂	3.3503	331
		33.9069	0.2371	65	2.6417	(101)	SnO ₂	2.6441	330
		41.2525	0.3006	221	2.1867	(101)	Mn	2.1871	266

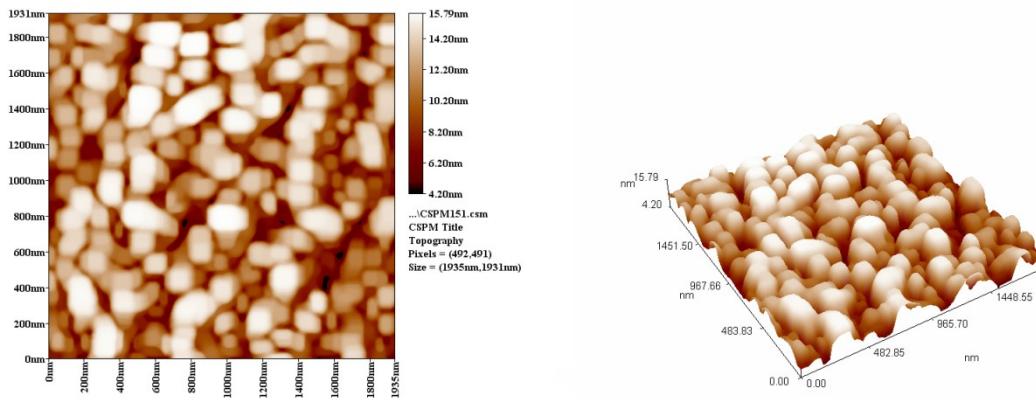
Table.1. Structural parameters of Mn doped SnO₂

The AFM images of SnO₂ /glass films pure and dopant with Mn sample were presented in Fig(2)The RMS roughness and the grain size have got correlation with the percentage of the doping concentrations of Mn (any increment in the in the percentage of doping there will be a relative increase value of the grain size). This consistent with Adawiya J. Haider et al. [22]





(c)



(d)

Fig (2): Illustrates the images of SnO₂ thin films pure and doping (30, 40 and 50)% concentration metal Mn with substrate temperature 200 °C a- SnO₂ pure b- SnO₂:30 %Mn c- SnO₂:40 %Mn d- SnO₂:50 %Mn concentrations

sample	grain size (nm)	RMS [nm] taken from 10×10 μm
SnO ₂ pure	84.55	1.392
SnO ₂ :30 % Mn	99.36	3.33
SnO ₂ :40 % Mn	103	3.43
SnO ₂ :50 % Mn	105	3.5

Table (2) Morphological characteristics of the SnO₂:Mn /glass thin films deposited at different doping concentration at Oxygen pressure 10⁻² mbar and 700mJ/cm² laser fluence at 473 K

SnO₂ thin films were successfully deposited onto glass substrate and the films were very transparent. This may be attributed by the formation of the Fermi level in the conduction band [11]. The absorption coefficient (α) and incident photon energy ($h\nu$) is related by the following equation [3]

$$(\alpha h\nu)^2 = A (h\nu - E_g) \dots \dots \dots (3)$$

Where A constant, E_g optical energy gap.. Fig (3) shows the variation of transmittance with the wave length for Mn_xSn_{1-x}O₂ thin films the variation of transmittance (T) with respect to the wavelength thin films with different doping levels(Mn). The maximum transmittance is 95% , 85% , 80% ,25% (700 nm), respectively for 50 wt.% Mn ,40 wt.% Mn ,30% Mn concentration and pure SnO₂ . The increase in transmittance is attributed to both the well-crystallized film and the pinhole free surface [24].

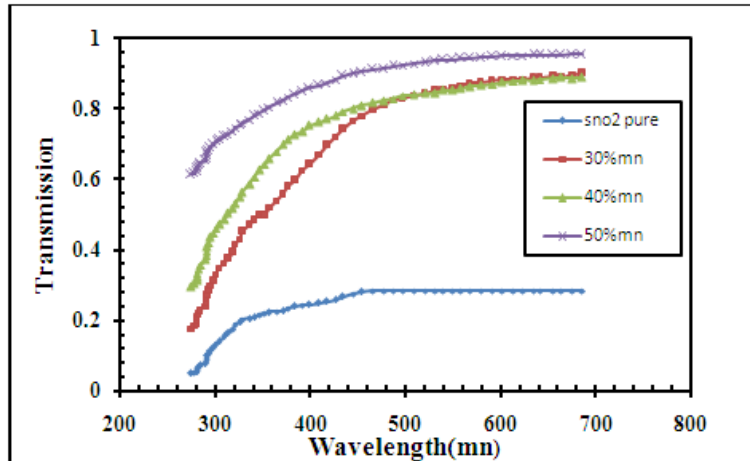


Fig (3) UV-VIS transmittance spectra of SnO₂:Mn films at different concentration

The optical energy gap values (E_g) for SnO₂ pure and doping with Mn films have been determined. A plot of $(\alpha h\nu)^2$ versus $h\nu$ for films with different doping concentration at 473 k is shown in Fig. (4). The plot is linear indicating the direct band gap nature of the films. Extrapolation of the line to the $h\nu$ axis gives the band gap. Results showed an increase in the Mn content to 50 % resulted in a decrease in the band gap to about (2.15-1.75) eV, as shown in the fig (4). The decrease of E_g^o value can be related to the crystallinity of the thin film. This decrease in energy gap can be due to the prohibited impurities that led to the formation of donor levels within the energy gap near the conduction band. Thus will absorb photons of low energy, this is an agreement with Adawiya. J.Haider et al. [22]

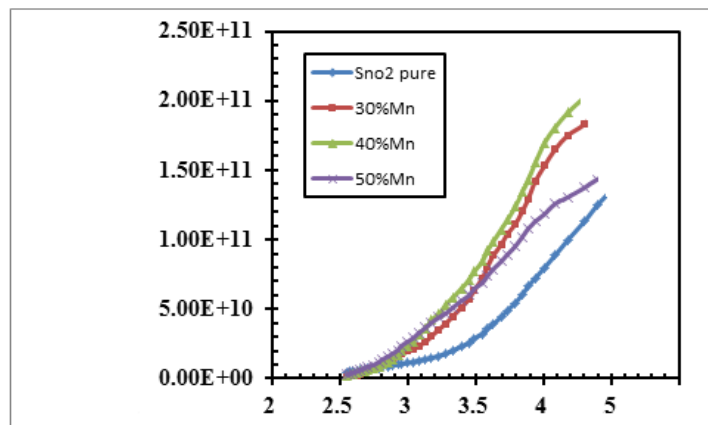


Fig (4) Optical band gap of SnO₂ pure and SnO₂:Mn films at different concentration
 a) SnO₂:30 % Mn b) SnO₂: 40% Mn c) SnO₂: 50% Mn

Samples	Optical energy gap (eV)
SnO ₂ pure	3.5
SnO ₂ :30%Mn	3.3
SnO ₂ :40%Mn	3.2
SnO ₂ :50%Mn	3.15

Table (3) the obtained result of optical energy gap of SnO₂ :Mn at different doping concentration At 473 k

Optical constants included refractive index (n), extinction coefficient (k), and real (ϵ_r) and imaginary parts (ϵ_i) of dielectric constant. The refractive index (n) can be calculated from the following equation. [4]

$$n = \left[\frac{4R}{(R-1)^2} - k^2 \right]^{1/2} - \frac{(R+1)}{(R-1)} \dots \dots \dots (4)$$

Where R is the reflectance and given by the equation.[5]

$$R = \frac{(n - 1)^2 + k^2}{(n + 1)^2 + k^2} \dots\dots\dots (5)$$

We can notice from figure (5) that the refractive index, in general increasing with doping concentration

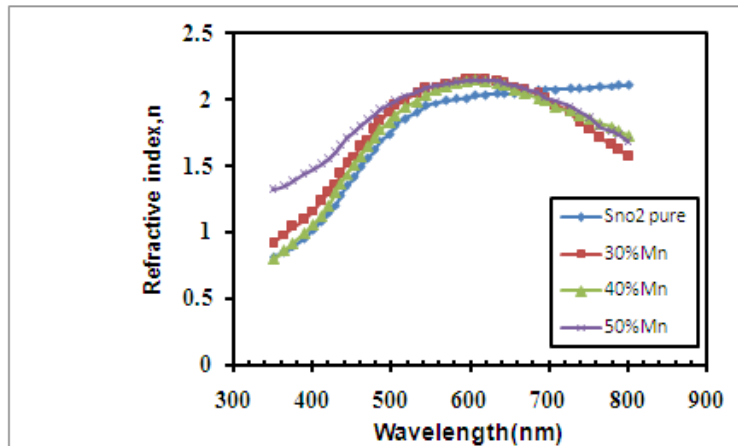


Fig (5) Variation of n with λ of the SnO₂:Mn /glass films at different doping concentration at 473 k

The behavior of the extinction coefficient (k) is nearly similar to the corresponding absorption coefficient as shown in Fig (6) at different doping concentration at 473 k We can observe from these figure and Table (4) and Fig.(6) that the extinction coefficient, in general, decreases with increasing of doping concentration for all films. This is attributed to the same reason mentioned previously in the absorption coefficient.

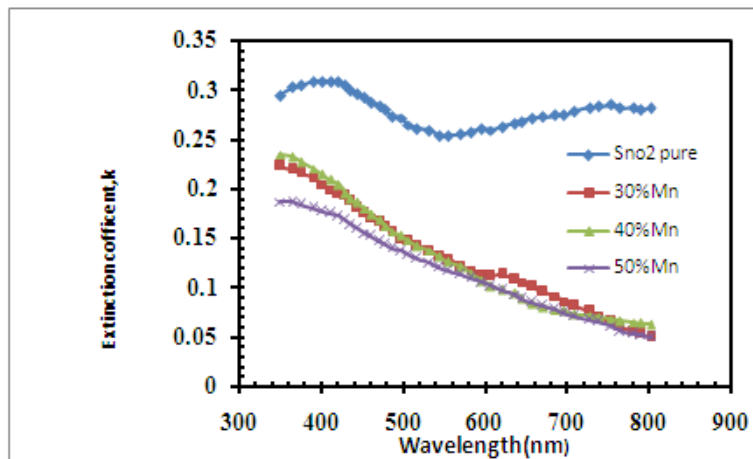


Fig (6) Variation of k with λ of the SnO₂:Mn /glass films at different doping concentration at 473 k

The variation of the real (ε_r) and imaginary (ε_i) parts of the dielectric constant values versus wavelength in the range 300 – 900nm at different concentration doping at annealing temperature (473)K and are shown in Fig(7) The behavior of ε_r is similar to that of refractive index because the smaller value of k² compared with n², while ε_i is mainly depends on the k values, which are related to the variation of absorption coefficient. It is found that ε_r and ε_i were increased with increasing of concentration doping

It is found that ε_r change from (3.4 to4.3) at different doped concentration while ε_i change from (0.5to1) at different doped concentration at 473 k

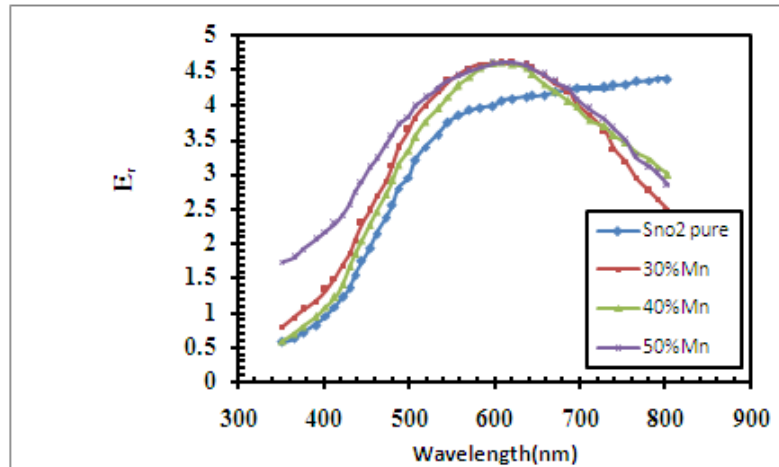


Fig (7-a) Variation of n_r with λ of the SnO₂:Mn /glass films at different doping concentration at 473 k

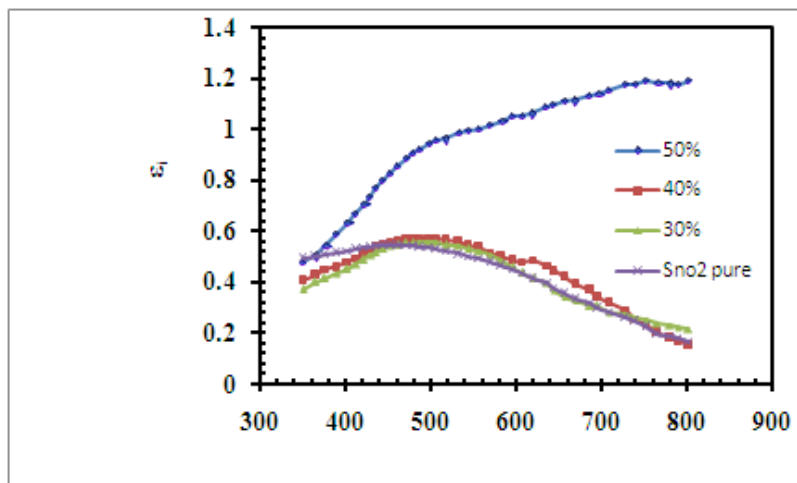


Fig (7-b) Variation of k_i with λ of the SnO₂:Mn /glass films at different doping concentration at 473 k

473 k	x	0%	30%	40%	50%
	E _g (eV)	3.5	3.3	3.2	3.15
	n	1.8	2	2.01	2.1
	k*10 ⁻³	0.26	0.14	0.13	0.12
	ε _r	3.4	3.9	3.7	4.2
	ε _i *10 ⁻²	1	0.6	0.55	0.5

Table (4) Parameters of the optical properties of SnO₂:Mn films at different doping concentration at 473 k

IV. Conclusion

Thin films of pure and antimony doped tin oxide were prepared On a glass substrate by pulse laser deposition . The effects of doping levels on the optical and structural properties of SnO₂: Mn For (200) nm thick at473k were experimentally investigated. XRD analysis shows that the sample for SnO₂ pure is nearly amorphous and all the samples are polycrystalline and Mn-doping affected the crystallinity disorder by increasing it .UV-VIS transmittance measurements have shown that our films are highly transparent in the visible wavelength region, with an average transmittance of ~90% which makes them suitable for sensor applications The surface morphology of the deposit materials have been studied by using scanning electron microscope and atomic force microscope. RMS roughness increased with increasing doping concentration

References:

- [1]. J. Joseph, V, K. E. Abraham, Chinese Journal of Physics, 45,No.1, 84 (2007).
- [2]. B. O'Regan, M. Grätzel, Nature 353 (1991) 737.
- [3]. H. Kim, G.P. Kushto, C.B. Arnold, Z.H. Kafafi, A. Pique, Appl. Phys. Lett.85 (2004) 464.
- [4]. T. Fukano, T. Motohiro, T. Ida, H. Hashizume, J. Appl. Phys. 97 (2005)084314.
- [5]. W. Brütting, M. Meier, M. Herold, S. Krag, M. Schwöerer, Chem. Phys.227 (1998) 243.
- [6]. C. Arias, L.S. Roman, T. Bugler, R. Tomfool, M.S. Moravia, I.A. Hummel, Thin Solid Films 371 (2000) 29.

- [7]. A. Rakhshani, Y. Makdish, H. Ramazaniyan, J. Appl. Phys. 83 (1998)1049.
- [8]. A. Martinez, D.R. Acosta, Thin Solid Films 483 (2005) 107.
- [9]. B. Thangaraju, Thin Solid Films, 402 (2002) 71.
- [10]. D. Das, R. Banerjee, Thin Solid Films 147 (1987) 321.
- [11]. O.K. Varghese, L.K. Malhotra, J. Appl. Phys. 87 (2000) 7457.
- [12]. Y. Onuma, Z. Wang, H. Ito, M. Nakao, K. Kamimura, Jpn. J. Appl. Phys. 37 (1998) 963.
- [13]. B.P. Howson, H. Barakova, A.G. Spencer, Thin Solid Films 196 (1991)315.
- [14]. B. Stjerna, E. Olsson, C.G. Granqvist, J. Appl. Phys. 76 (1994) 3797
- [15]. D.B. Chrisey, G.K. Hubler, Pulsed Laser Deposition of Thin Films, Wiley, New York, 1994.
- [16]. H. Kim, C.M. Gilmore, A. Piqué, J.S. Horwitz, H. Mattoussi, H. Murata, Z.H. Kafafi, D.B. Chrisey, J. Appl. Phys. 86 (1999) 6451.
- [17]. H. Kim, J.S. Horwitz, G. Kushto, Z.H. Kafafi, D.B. Chrisey, Appl. Phys. Lett. 79 (2001) 284
- [18]. Joint Committee on Powder Diffraction Standards, International Centre for Diffraction Data, # 41-1445.
- [19]. S. H. Jeong, B. N. Park, S. B. Lee and J.-H. Boo, " Structural and optical properties of silver-doped zinc oxide sputtered films ", Surface & Coatings Technology, Vol. 193, PP.340– 344, (2005). **r and**
- [20]. C.H. Liu, L. Zhang, Yuan-Jin He, "Properties and Mechanism Study of Ag Doped SnO₂ Thin Films As H₂S Sensors", Thin solid Film, Vol. 304, PP.13-15, (1997).
- [21]. J. Langford and A. Wilson, " J.Appl.Cryst. ", No.11, (1978),P.102
- [22]. Adawiya J.Haider, Khalid. A. Sukar, Khaled. Z. Yahya," Ag Doped Tin-Oxide Laser Deposition (PLD)", Journal of the college of the education in the sixth conference on physics, Vol.3, (2009), p.181- 189
- [23]. C.Kilic & A.Zunger. (2002). Origins of coexistence of conductivity and transparency in SnO₂Physics Review Letters: 88. 095501
- [24]. A V Moholkar, S M Pawara, K Y Rajpure, C H Bhosale and J H Kim, Appl. Surface Sci. **255**, 9358 (2009)